

Impact of Amino-Functionalization on the Response of Poly(ethylene glycol) (PEG) to External Stimuli

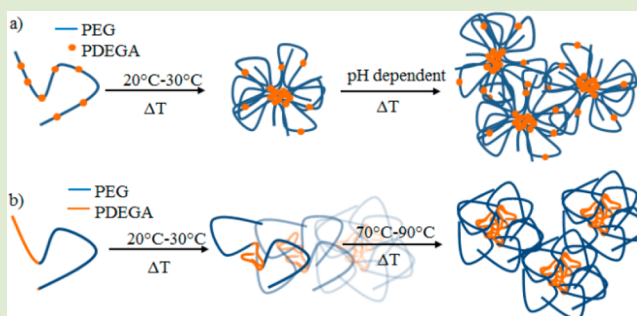
Dennis Kurzbach,[†] Valerie S. Wilms,[‡] Holger Frey,[‡] and Dariush Hinderberger^{*,†}

[†]Max Planck Institute for Polymer Research, Ackermannweg 10, 55128 Mainz, Germany

[‡]Department of Organic Chemistry, Johannes Gutenberg-University Mainz, Duesbergweg 10-14, 55128 Mainz, Germany

Supporting Information

ABSTRACT: It is shown that amino-functionalization of poly(ethylene glycol) (PEG) with the comonomer *N,N*-diethyl glycidyl amine (DEGA) triggers the emergence of extraordinary stimuli responsiveness and phase behavior of PEG. In dependence of the solution pH, tapered PEG-*co*-PDEGA exhibits a highly cooperative two-step inverse phase transition with respect to temperature. The polymer forms dispersed metastable nanoglobules in the medically relevant temperature range around human body temperature. Independently, cloud points can be adjusted between 40 and 90 °C via the pH of the solution. Changing the polymer architecture to a block structure, in pronounced contrast, the polymer exhibits a gradual growth of micelles with temperature until macroscopic aggregation takes place. Thus, through amino-functionalization of PEG, one can precisely control the temperature range and the mechanism of the inverse phase transition of this promising polymer-therapeutics candidate by adjusting solution conditions and polymer topology.



In recent years, astonishing developments have been achieved in the field of polymer-based systems for therapeutic applications, like in targeted drug delivery.¹ In this context, one of the most promising structures is poly(ethylene glycol) (PEG), because it does not exhibit immunogenicity, antigenicity, and toxicity.^{2–5} However, until recently, the applicability of PEG was limited by its lack of functional groups, prohibiting, for example, drug conjugation. Yet, the recent developments in anionic ring-opening polymerization opened up new routes toward functionalized PEG,^{2–5} allowing for versatile usage in modern therapeutic strategies.⁶ Drug accumulation in tumor tissue based on hyperthermia or pH irregularity becomes possible by tuning the stimuli responsiveness of functional polyethers.^{7–9} It is apparent that many properties of these state-of-the-art structures are so far undiscovered and that there is demand for innovative experimental techniques and theoretical concepts to gather deeper understanding of their complex response to external stimuli. This is a prerequisite for purposeful synthesis and directed application of systems for polymer therapeutics.

In this work, we aim at showing that the newly available^{10,11} slightly tapered copolymer poly(ethylene glycol)-*co*-poly(*N,N*-diethyl glycidyl amine) (PEG-*co*-PDEGA; see Figure 1a) and its block-structured analogue PEG-*b*-PDEGA exhibit surprising temperature and pH dependences in the temperature range around human body temperature, between 25 and 45 °C. The latter temperature represents the upper limit of therapeutic hyperthermia, which highlights the potential importance for medical applications.¹² We demonstrate that the combination

of intrinsically local continuous wave electron paramagnetic resonance (CW EPR) spectroscopy and macroscopic turbidimetry reveals an astonishing versatility and complexity of the temperature-induced inverse phase transition of PEG-*co*-PDEGA and PEG-*b*-PDEGA. We find that the polymers form soluble nanoaggregates capable of incorporating large amounts of, like most low-molecular drugs, amphiphilic guest molecules between 20 and 30 °C, with the number of incorporated guests depending on the solution pH. Macroscopically observable large-scale aggregation and subsequent precipitation takes place at significantly higher temperatures (up to 50 °C higher). While PEG-*b*-PDEGA nanoscopically features a more continuous phase transition (non-first-order, like it is known for homo-PEG¹³) PEG-*co*-PDEGA surprisingly exhibits a high degree of cooperativity, indicating a first order nanophase transition.^{8,14} The cloud points of the latter system can furthermore be tuned, largely independent of the nanoaggregate formation by adjusting the environmental pH. Thus, amino-functionalization of PEG leads to the emergence of intriguing phase transition modes of an otherwise rather simple and widely used polymer that are highly interesting from a materials science and polymer physics point of view.

To gain deeper understanding of the temperature-dependence of the nanoscale solution behavior of PEG-*co*-PDEGA (tapered copolymer with 29% DEGA and a molecular weight of

Received: November 9, 2012

Accepted: January 14, 2013

Published: January 17, 2013

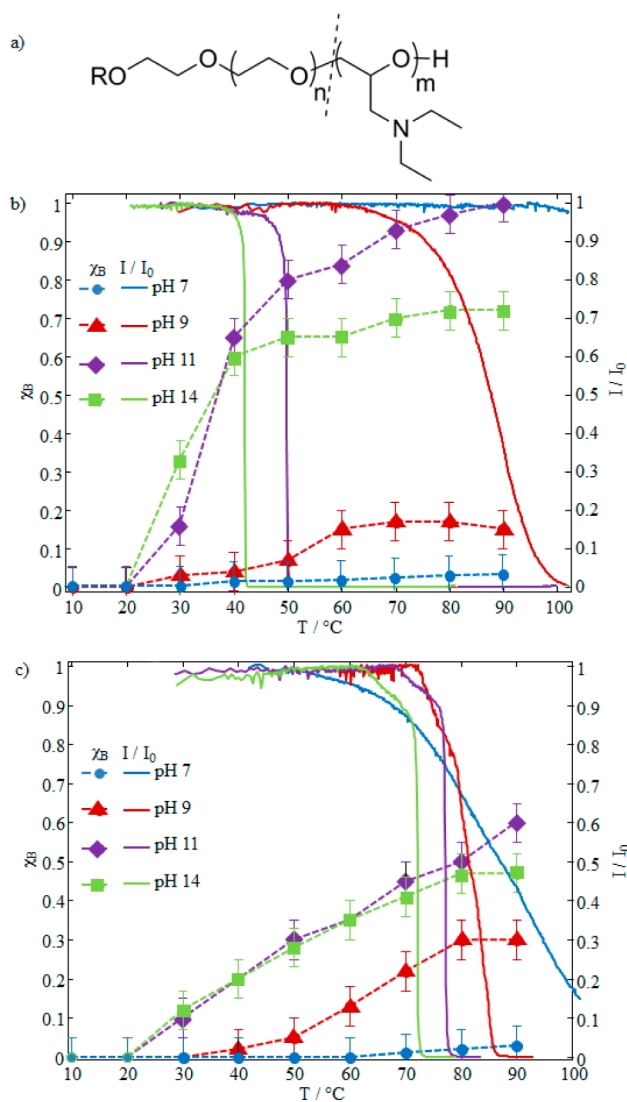


Figure 1. (a) Molecular structure of PEG-co-PDEGA/PEG-b-PDEGA. (b) Fraction of TEMPO incorporated into collapsed PEG-co-PDEGA domains, χ_B , as function of temperature for different pH (symbols connected by dashed lines). The corresponding turbidity measurements of the solutions (transmitted light intensity, I/I_0 , respectively) are shown as solid lines (see legend). All measurements were performed at 5 wt % polymer concentration. (c) The fraction of TEMPO incorporated into collapsed PEG-b-PDEGA domains, χ_B , and the transmitted intensity as a function of temperature for different pH. The color code is the same as in (a). Error bars denote uncertainties in spectral simulations (see the Supporting Information).

3300 g mol⁻¹) and PEG-b-PDEGA (block copolymer with 22% DEGA and a molecular weight of 6600 g mol⁻¹), we performed temperature-dependent CW EPR measurements at different pH on 0.2 mM of the small and (like most drugs¹⁵) amphiphilic spin probe TEMPO ((2,2,6,6-tetramethylpiperidin-1-yl)oxyl). The probe reports the occurrence of collapsed, polymer-rich domains on the nanoscale (the polymer concentration was 5 wt %).^{16–18} If TEMPO becomes partitioned between such a domain and the aqueous environment, one observes two spectral signatures, from probes in the aqueous environment (species A) and in water-depleted, collapsed/polymer-rich domains (species B).

The fraction of TEMPO incorporated into polymer-rich domains can be quantified by its mole fraction $\chi_B = n_B / \sum_i n_i$

(see the SI for a detailed description of the CW EPR spin-probing approach). As can be observed in Figure 1b), in solutions of PEG-co-PDEGA, species B occurs (rising χ_B) in the narrow temperature range between 20 and 30 °C at pH 9, 11, and 14. Only at pH 7, the contribution of species B is very small, such that it is hard to determine the temperature range in which species B occurs with the same accuracy. Nonetheless, in any case, PEG-co-PDEGA shows a thermal response and collapses when exposed to heat, as proven by $\chi_B > 0$ (note that linear homo-PEG does not give rise to any changes in χ_B or turbidity under the present conditions).¹⁰ Yet, the fraction of species B at a given temperature varies drastically with pH, as a consequence of changing hosting parameters with changing degree of DEGA protonation. Interestingly, for pH 11, $\chi_B = 1$ at 90 °C, which translates to complete uptake of TEMPO probes. At the concentrations used, this has so far not been observed for any other thermoresponsive system that has been investigated by means of CW EPR.^{16,19}

When inspecting the degree of protonation, the narrowness of the temperature range in which collapsed domains initially occur (between pH 9 and 14: 20–30 °C) is quite unexpected, because changes in pH alter the chemical structure of the polymer. The pK_a of PEG-co-PDEGA is around 10 (see the Supporting Information). Such, for the percentage of protonated amines, one obtains pH 7: >99.9%; pH 9: ~90%; pH 11: ~10%; pH 14: <0.1%. Thus, one would expect differences in hydration energy and hence strong effects on the collapse temperature. This is qualitatively not the case here. In this context it is important to note that spin-probing CW EPR is only dependent on local structures on length scales of a few nanometers. Hence, because at any pH (varying) fractions of nonprotonated DEGA units are distributed along the polymer chains, it is very likely that the local polymer collapse on length scales below approximately 2 nm is always triggered by chemically equivalent segments of deprotonated PDEGA and PEG (similar phenomena have been observed recently^{16,19}).

Intriguingly, the turbidity of the PEG-co-PDEGA solutions remains unchanged if the temperature does not exceed 40 °C, although structures appear that are large enough to host a significant amount of TEMPO as the temperature rises above 20–30 °C: more than 50% of the probe molecules at pH 11 and 14; see Figure 1b). Thus, one can conclude that PEG-co-PDEGA forms small nanoaggregates (likely of globular shape¹⁹) or similar structures that are too small to scatter light and that remain dissolved at intermediate temperatures (no increase in turbidity was observed for longer waiting periods). The mean-square diffusional displacement of the TEMPO probes at 40 °C is $(\langle x_T^2 \rangle)^{1/2} \approx 3.5$ nm at pH 11 and $(\langle x_T^2 \rangle)^{1/2} \approx 2.8$ nm at pH 14 (see ref 20 and the Supporting Information for details). In addition, we do not observe dynamic probe exchange between the collapsed domains and the solvent-exposed regions. Taken together, one may estimate the radius of the aggregates to ~5–10 nm from CW EPR. This estimation is independently substantiated by dynamic light scattering data that yields an average hydrodynamic radius of the nanoaggregates of ~9 nm at 40 °C (see the Supporting Information). In contrast at 25 °C, where $\chi_B = 0$ and, hence, all polymers are individually dissolved, the unimers exhibit an average hydrodynamic radius of ~2 nm.

In this context, the sigmoidal and steep development of the χ_B functions is clearly indicative of a high degree of cooperativity for the nanoaggregate formation.¹⁴ Because dehydration of PEG typically is a noncooperative process,⁸

we assume as underlying reason for the observed cooperativity that some of the randomly distributed deprotonated, hydrophobic¹⁹ DEGA moieties can always be found on the surface of any collapsed structure of PEG-*co*-PDEGA. Increased concentration of such surface moieties may well facilitate the attraction of still swollen PEG-*co*-PDEGA. Thus, a cooperative and nanoscale sharp transition can be observed, making it even more interesting that the nanoaggregates remain macroscopically solvated below 40 °C. This explanation is also in agreement with the fact that at pH 9 no cooperative aggregation can be observed: too many DEGA units are charged for an effective hydrophobic attraction of nearby polymers.

Only as the temperature rises above 42 °C, the turbidity of the PEG-*co*-PDEGA solutions increases at pH 14, indicating metastability of the nanoaggregates (see Figure 1b). Yet, at 30 °C, no changes in turbidity were observed even over hours. The cloud point, T_c , in contrast to the nanoaggregate formation, is dependent on the solution pH to a certain degree and can be shifted from 42 °C at pH 14 to 85 °C at pH 9. Note that the cloud points as well as the temperature of first occurrence of TEMPO species B are largely independent of the polymer concentration.²⁰ At pH 7, changes in turbidity could not be detected, likely as a consequence of charged DEGA groups keeping the polymer solvated and elongated. Because no abrupt changes in χ_B can be observed at the cloud points at different pH, one can deduce that the initially formed nanoscopic aggregates cluster to form large structures at T_c and do not rearrange into other conformations. Because T_c decreases with increasing pH, it is at hand to assume that deprotonation of the DEGA units and accompanying loss of coordinating water molecules leads to lower solvation energy of the PEG-*co*-PDEGA nanoaggregates (the loss of solvating water with increasing pH is also reflected in the CW EPR spectra, as shown in the Supporting Information). Note that also this second transition step, the clustering of nanoaggregates, exhibits a high degree of cooperativity at pH 11 and 14, likely again due to surface-exposed DEGA moieties.

The picture of the temperature-induced phase transition of PEG-*co*-PDEGA that arises from our data is schematically depicted in Figure 2a). In a first step, metastable nanoaggregates occur, which remain dissolved, that is, the solutions remain clear. The aggregates are depicted with the hydrophobic

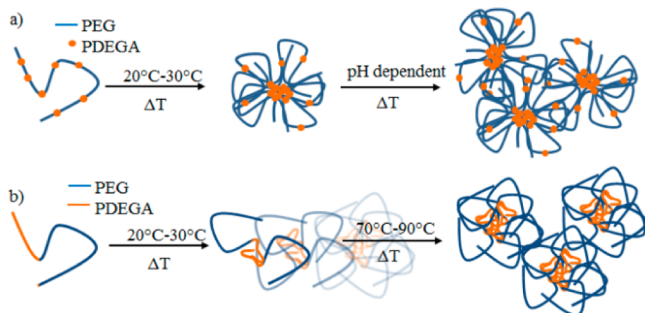


Figure 2. Schematic depiction of the temperature-triggered phase transitions. (a) PEG-*co*-PDEGA: Initially small aggregates are formed and remain dissolved. This occurs between 20 and 30 °C. In a second step, the aggregates cluster to form large structures. The aggregation temperature can be shifted from 42 to 85 °C by adjusting the pH. (b) PEG-*b*-PDEGA: above 20–30 °C, micelles grow steadily until they aggregate between 70 and 90 °C.

DEGA units clustered in the center, which is a likely conformation for amphiphilic random copolymers.^{19,21–23} If the temperature is further increased, the nanoscopic aggregates cluster in a second step to form large structures that precipitate. The first step takes place in a confined temperature range with respect to pH, while the second is more strongly dependent on pH. Interestingly, both steps of the phase transition of PEG-*co*-PDEGA are very sharp at pH 11 and 14, while conventional PEG normally features a rather broad transition range.⁸ This is indicative for a high degree of cooperativity and highlights the impact of amino-functionalization on the physicochemical properties of PEG.

Like for PEG-*co*-PDEGA, the nanoscale collapse of its block-structured analogue, PEG-*b*-PDEGA, sets in between 20 and 30 °C at pH 9, 11, and 14. Yet, in contrast to PEG-*co*-PDEGA, χ_B grows steadily until a temperature of 80 °C is reached (Figure 1c), indicating a noncooperative nanophase separation. Collapsed domains grow steadily, resulting in a growing volume fraction of water-depleted regions that entrap TEMPO molecules. Notably, again no changes in turbidity can be observed until higher temperatures are reached, suggesting that the formed objects are of small nanoscopic size and remain solvated at intermediate temperatures ($(\chi_T^2)^{1/2} \approx 3.0$ nm for species B for both pH 11 and 14 at 80 °C). Only between 70 and 90 °C, these nanoaggregates cluster to form larger structures, as can be deduced from the turbidimetry curves in Figure 1c). The turbidity does not decrease as steeply with temperature as for PEG-*co*-PDEGA at pH 11 and 14 (initially small slope of I/I_0), indicating a lower degree of cooperativity not only of the nanoscale collapse (see the slopes of the χ_B functions), but also of the macroscopically detectable aggregation step in the case of block architecture. This lack in cooperativity of the phase transition and the more “PEG-like” behavior of PEG-*b*-PDEGA is likely a consequence of the block architecture: DEGA blocks form the core of PEG-*b*-PDEGA aggregates (probably unimers initially), while the PEG blocks build the corona (depicted in Figure 2b).²⁰ Such, the DEGA units are screened by the PEG coronas not allowing for effective attraction of swollen PEG-*b*-PDEGA molecules (for the local collapse) or nanoaggregates (for macroscopic aggregation), hampering DEGA-mediated cooperativity. This is also in good agreement with the observation that the average fraction of incorporated TEMPO is much smaller for PEG-*b*-PDEGA than for PEG-*co*-PDEGA, because different aggregate conformations are very likely to yield differently favorable environments for TEMPO probes. Note that this is in good agreement with our earlier observation that more densely packed structures like ordered core–shell-type micelles incorporate less amphiphiles than randomly arranged aggregates of amphiphilic random copolymers.¹⁹ At pH 7, no significant interaction between TEMPO and PEG-*b*-PDEGA can be observed by means of CW EPR, but a very broad turbidity transition is detected that crosses the other three turbidity functions (Figure 1c). This phenomenon is a consequence of the formation of inverse micelles: since at pH 7 most of the DEGA units are charged, they constitute the corona of PEG-*b*-PDEGA aggregates, while PEG forms the core and now triggers the thermal response. Thus, a broad transition-temperature range is observed, which is typical for PEG.⁸

It is noteworthy that the onset of the nanophase separation (EPR) and the macroscopically visible aggregation of PEG-*b*-PDEGA (turbidity) are separated by more than 50 °C. In a very

wide temperature range, the block-copolymer forms nanoaggregates that remain dissolved, while for PEG-*co*-PDEGA, the nanoscopic and macroscopic collapse temperatures are significantly closer (see Figure 1). To the best of our knowledge, such drastic differences between the nanoscale collapse of a polymer and the macroscopic aggregation has not been achieved to date. The general phase transition mode of PEG-*b*-PDEGA is schematically shown in Figure 2b). As for its slightly tapered analogue the phase transition begins in the narrow temperature range between 20 and 30 °C at any pH. Yet in contrast to PEG-*co*-PDEGA, PEG-*b*-PDEGA aggregates grow steadily, until the cloud point is reached, at which the aggregates themselves cluster and precipitate.

Hosting amphiphilic structures like TEMPO without precipitation is an unusual and desirable property of polymers for drug transport through body fluid. Drugs could be transported in solution, while not being subject to proteolytic degradation. Obviously PEG-*co*-PDEGA and PEG-*b*-PDEGA are good examples of the versatility of functional PEG for future drug-delivery applications. Furthermore, the second step of the temperature-induced phase transition of these versatile structures could be exploited to accumulate polymer-drug conjugates in tissue that is subject to hyperthermia and pH irregularities, although in the present state precipitation within the temperature range achievable through hyperthermia is only observed at pH 14. This discrepancy, however, may well be overcome by adjusting the molecular weight of either types of the polymer or by incorporating a higher fraction of DEGA units, which is currently on the agenda in our laboratories.

Altogether we have shown that amino-functionalization of PEG in combination with a specific copolymer topology can lead to the emergence of previously unexpected physicochemical properties that allow for precise manipulation of very complex phase transition modes by adjusting the environmental conditions. Our study shows that extensive understanding of the phase behavior of advanced stimuli-responsive polymers, which is necessary to estimate the in-vivo behavior of a hosting system, demands for the combination of macroscopic methods with intrinsically local observation techniques.

■ ASSOCIATED CONTENT

■ Supporting Information

Experimental procedures, details on the spin-probing approach, spectral data and simulations, titration, and light scattering data. This material is available free of charge via the Internet at <http://pubs.acs.org>.

■ AUTHOR INFORMATION

Corresponding Author

*E-mail: dariush.hinderberger@mpip-mainz.mpg.de.

Notes

The authors declare no competing financial interest.

■ ACKNOWLEDGMENTS

We thank Christian Bauer for technical support and Prof. Hans W. Spiess for continuing support. D.K. and V.S.W. acknowledge support by the Gutenberg Academy of the University of Mainz. V.S.W. is thankful to the Graduate School "Materials Sciences in Mainz" for financial support and to the "Fonds der Chemischen Industrie". This work was financially supported by Max Planck Graduate Center with the University of Mainz (MPGC) and the Deutsche Forschungsgemeinschaft (DFG)

under Grant Number HI 1094/2-1 and through the "Sonderforschungsbereich" SFB 625.

■ REFERENCES

- (1) Duncan, R. *Nat. Drug Discovery Rev.* **2003**, *2*, 347–360.
- (2) Obermeier, B.; Wurm, F.; Mangold, C.; Frey, H. *Angew. Chem., Int. Ed.* **2011**, *50*, 7988–7997.
- (3) Weber, C.; Hoogenboom, R.; Schubert, U. S. *Prog. Polym. Sci.* **2012**, *37*, 686–714.
- (4) Knop, K.; Hoogenboom, R.; Fischer, D.; Schubert, U. S. *Angew. Chem., Int. Ed.* **2010**, *49*, 6288–6308.
- (5) Mangold, C.; Wurm, F.; Frey, H. *Polym. Chem.* **2012**, *3*, 1714–1721.
- (6) Barner-Kowollik, C.; Lutz, J.-F.; Perrier, S. *Polym. Chem.* **2012**, *3*, 1677–1679.
- (7) Schömer, M.; Seiwert, J.; Frey, H. *ACS Macro Lett.* **2012**, *1*, 888–891.
- (8) Aseyev, V.; Tenhu, H.; Winnik, F. M. *Adv. Polym. Sci.* **2011**, *242*, 29–89.
- (9) Mangold, C.; Obermeier, B.; Wurm, F.; Frey, H. *Macromol. Rapid Commun.* **2011**, *32*, 1930–1934.
- (10) Reuss, V. S.; Obermeier, B.; Dingels, C.; Frey, H. *Macromolecules* **2012**, *45*, 4581–4589.
- (11) Reuss, V. S.; Werre, M.; Frey, H. *Macromol. Rapid Commun.* **2012**, *33*, 1556–1561.
- (12) Hahn, G. M. *Cancer Res.* **1979**, *39*, 2264–2268.
- (13) Matsuyama, A.; Tanaka, F. *Phys. Rev. Lett.* **1990**, *65*, 341–344.
- (14) Holde, K. E. v.; Johnson, W. C.; Ho, P. S. *Principles of Physical Biochemistry*; Prentice Hall: NJ, 1998.
- (15) Bemis, G. W.; Murcko, M. A. *J. Med. Chem.* **1996**, *39*, 2887–2893.
- (16) Kurzbach, D.; Reh, M. N.; Hinderberger, D. *ChemPhysChem* **2011**, *12*, 3566–3572.
- (17) Junk, M. J. N.; Jonas, U.; Hinderberger, D. *Small* **2008**, *4*, 1485–1493.
- (18) Junk, M. J. N.; Li, W.; Schlüter, A. D.; Wegner, G.; Spiess, H. W.; Zhang, A.; Hinderberger, D. *Macromol. Chem. Phys.* **2011**, *212*, 1229–1235.
- (19) Kurzbach, D.; Wilms, V. S.; Schömer, M.; Frey, H.; Hinderberger, D. *Macromolecules* **2012**, *45*, 7535–7548.
- (20) Junk, M. J. N.; Li, W.; Schlüter, A. D.; Wegner, G.; Spiess, H. W.; Zhang, A.; Hinderberger, D. *Angew. Chem., Int. Ed.* **2010**, *122*, 5818–5823.
- (21) Chee, C. K.; Rimmer, S.; Shaw, D. A.; Soutar, I.; Swanson, I. *Macromolecules* **2001**, *34*, 7544–7549.
- (22) Zhang, G.; Winnik, F. M.; Wu, C. *Phys. Rev. Lett.* **2003**, *90*, 35506–35501.
- (23) Borisov, O. V.; Halperin, A. *Macromolecules* **1996**, *29*, 2612–2617.